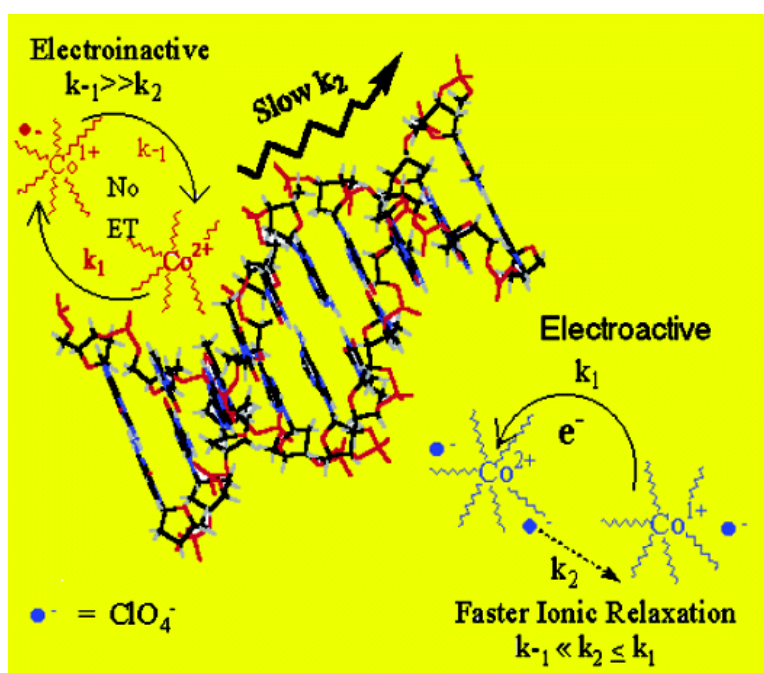


Ion Atmosphere Relaxation and Percolative Electron Transfer in Co Bipyridine DNA Molten Salts

Anthony M. Leone, Jennifer D. Tibodeau, Steven H. Bull,
 Stephen W. Feldberg, H. Holden Thorp, and Royce W. Murray

J. Am. Chem. Soc., **2003**, 125 (22), 6784-6790 • DOI: 10.1021/ja0348795 • Publication Date (Web): 13 May 2003

Downloaded from <http://pubs.acs.org> on March 29, 2009



More About This Article

Additional resources and features associated with this article are available within the HTML version:

- Supporting Information
- Links to the 1 articles that cite this article, as of the time of this article download
- Access to high resolution figures
- Links to articles and content related to this article
- Copyright permission to reproduce figures and/or text from this article

[View the Full Text HTML](#)

Ion Atmosphere Relaxation and Percolative Electron Transfer in Co Bipyridine DNA Molten Salts

Anthony M. Leone, Jennifer D. Tibodeau, Steven H. Bull, Stephen W. Feldberg, H. Holden Thorp,* and Royce W. Murray*

Contribution from the Kenan Laboratories of Chemistry, University of North Carolina, Chapel Hill, North Carolina 27599-3290

Received February 26, 2003; E-mail: holden@unc.edu; rwm@email.unc.edu

Abstract: Polypyridyl complexes of Co decorated with 350-Da polyether chains (Co_{350}^{2+}) form molten phases of nucleic acids when paired with DNA counterions ($\text{Co}_{350}\text{DNA}$) or 25-mer oligonucleotides. Analysis of voltammetry and chronoamperometry of mixtures of these phases with complexes having ClO_4^- counterions ($\text{Co}_{350}(\text{ClO}_4)_2$) and no other diluent provides charge transport rates from the oxidation and reduction currents for the complexes. As the mole fraction of the $\text{Co}_{350}(\text{ClO}_4)_2$ complex in the mixture is varied from ca. 0.25 to 1, the physical diffusion constants derived from the Co^{III} wave increase from $1 \times 10^{-11} \text{ cm}^2/\text{s}$ to $5 \times 10^{-10} \text{ cm}^2/\text{s}$, and apparent diffusion constants dominated by the Co^{II} electron self-exchange increase from $1 \times 10^{-10} \text{ cm}^2/\text{s}$ to $2 \times 10^{-8} \text{ cm}^2/\text{s}$. Pure $\text{Co}_{350}\text{DNA}$ melts, containing no $\text{Co}_{350}(\text{ClO}_4)_2$ complex, do not exhibit recognizable voltammetric waves; DNA suppresses the Co^{II} electron transfer reactions of Co complexes for which it is the counterion. There are therefore two microscopically distinct kinds of Co_{350} complexes, those with DNA and those with ClO_4^- counterions, with respect to their Co^{II} electron-transfer dynamics, leading to percolative behavior in their mixtures. The electron-transfer rates of the Co^{II} couple are controlled by the diffusive relaxation of the ionic atmosphere around the reaction pair, and the inactivity of the bound Co complexes can be attributed to the very low mobility of the anionic phosphate groups in the DNA counterion. Substitution of sulfonated polystyrene for DNA produced similar results, suggesting that this phenomenon is general to other polymer counterions of low mobility. We conclude that the measured Co^{II} charge transport and electron-transfer rate constants reflect more the diffusive mobility of the perchlorate counterion than the intrinsic Co^{II} electron hopping rate.

Studies of mass and electron transport in semisolids provide fundamental information about electron-transfer reactions.¹ Liquid and glassy phases that are suited for such investigations can be obtained through synthetic addition of short polyether tails to redox-active molecules.^{2–4} Because these phases are comprised wholly of redox-active molecules, mass and electron transport in them are most readily evaluated electrochemically. The possibilities for using DNA's molecular recognition properties for self-assembly,⁵ computing,⁶ and wiring⁷ has recently

prompted us to develop DNA molten salts⁸ as a step toward achieving guided functions within the ionically and electronically conductive melt environment. We desired to demonstrate electronic communication⁹ with the DNA as well as to arrive at a fuller understanding of the influence of the DNA on the physical and electronic properties of the materials. Our initial publication⁸ briefly addressed both of these topics. We now describe the influence of the DNA on the electrochemical properties of the materials.

A redox active DNA melt can be comprised of polyether-decorated metal trisbipyridine cations and nucleic acid anions. Other anions and poly-anions can also be employed. The compounds in Figure 1 are room-temperature molten salts^{2–4} composed of a Co(II) tris-bipyridine complex in which the ligands bear oligomeric methyl-terminated poly(ethylene glycol) chains ("PEG tails"). "X" represents the counterion of the metal

- (1) Terrill, R. H.; Murray, R. W. In *Molecular Electronics*; Jortner, J., Ratner, M. A., Eds.; Blackwell Science: Oxford, U.K., 1997.
- (2) Williams, M. E.; Masui, H.; Long, J. W.; Malik, J.; Murray, R. W. *J. Am. Chem. Soc.* **1997**, *119*, 1997–2005.
- (3) Masui, H.; Murray, R. W. *Inorg. Chem.* **1997**, *36*, 5118 (b) Velazquez, C. S.; E., H. J.; Murray, R. W. *J. Am. Chem. Soc.* **1993**, *115*, 7896 (c) Pinkerton, M. J.; LeMest, Y.; Zhang, H.; Watanabe, M.; Murray, R. W. *J. Am. Chem. Soc.* **1990**, *112*, 3730 (d) Longmire, M. L.; Watanabe, M.; Zhang, H.; Wooster, T. T.; Murray, R. W. *Anal. Chem.* **1990**, *62*, 747.
- (4) Long, J. W.; Velazquez, C. S.; Murray, R. W. *J. Phys. Chem. A* **1996**, *100*, 5492–5499.
- (5) Mirkin, C. A. *Inorg. Chem.* **2000**, *39*, 2258–2272 (b) Elghanian, R.; Storhoff, J. J.; Mucic, R. C.; Letsinger, R. L.; Mirkin, C. A. *Science* **1997**, *277*, 1078–1081.
- (6) Adelman, L. M. *Science* **1994**, *266*, 1021–1024 (b) Pirrung, M. C.; Connors, R. V.; Odenbaugh, A. L.; Montague-Smith, M. P.; Walcott, N. G.; Tollett, J. J. *J. Am. Chem. Soc.* **2000**, *122*, 1873–1882 (c) Braich, R. S.; Chelyapov, N.; Johnson, C.; Rothmund, P. W. K.; Adelman, L. *Science* **2002**, *296*, 499–502.
- (7) Porath, D.; Bezryadin, A.; de Vries, S.; Dekker: C. *Nature* **2000**, *403*, 635–638 (b) Fink, H. W.; Schonenberger, C. *Nature* **1999**, *398*, 407–410 (c) Mirkin, C. A.; Taton, T. A. *Nature* **2000**, *405*, 626–627.

- (8) Leone, A. M.; Weatherly, S. C.; Williams, M. E.; Thorp, H. H.; Murray, R. W. *J. Am. Chem. Soc.* **2001**, *123*, 218–222.
- (9) Johnston, D. H.; Glasgow, K. C.; Thorp, H. H. *J. Am. Chem. Soc.* **1995**, *117*, 8933–8938 (b) Johnston, D. H.; Thorp, H. H. *J. Phys. Chem.* **1996**, *100*, 13 837–13 843 (b) Hall, D. B.; Holmlin, R. E.; Barton, J. K. *Nature* **1996**, *382*, 731–735 (c) Armistead, P. M.; Thorp, H. H. *Anal. Chem.* **2000**, *72*, 3764–3770 (d) Armistead, P. M.; Thorp, H. H. *Anal. Chem.* **2001**, *73*, 558–564 (e) Eckhardt, A.; Espenhahn, E.; Napier, M.; Popovich, N.; Thorp, H.; Witwer, R. In *DNA Arrays: Technologies and Experimental Strategies*; Grigorenko, E. V., Ed.; CRC Press: Boca Raton, 2001; pp 39–60 (f) Schuster, G. B. *Acc. Chem. Res.* **2000**, *33*, 253–260.

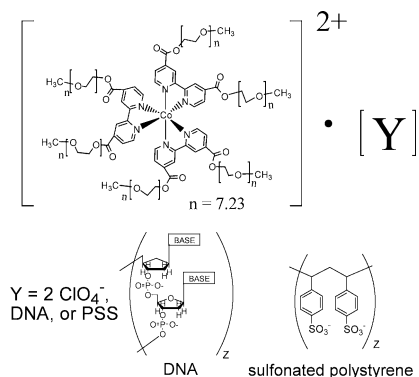


Figure 1. Co_{350}Y where $\text{Y} = 2 \text{ClO}_4^-$ for $\text{Co}_{350}(\text{ClO}_4)_2$, Y is a DNA base pair for $\text{Co}_{350}\text{DNA}$, $\text{Y} = 2$ sulfonate groups of sulfonated polystyrene for $\text{Co}_{350}\text{PSS}$.

complex and can be as follows: (a) two perchlorate anions, (b) two phosphate anions of a highly polymerized DNA molecule or of selected 25-mer oligonucleotides, or (c) two sulfonate groups of sulfonated polystyrene (PSS). These highly viscous, semisolid materials are succinctly abbreviated as follows: (a) $\text{Co}_{350}(\text{ClO}_4)_2$, (b) $\text{Co}_{350}\text{DNA}$, and (c) $\text{Co}_{350}\text{PSS}$, respectively. Using microelectrodes, it is possible to carry out voltammetric experiments in the undiluted molten salts of $\text{Co}_{350}(\text{ClO}_4)_2$, $\text{Co}_{350}\text{-DNA}$, $\text{Co}_{350}\text{PSS}$, and their mixtures, according to previously reported methods.^{2–4}

This paper describes the transport and electron-transfer properties of mixtures of $\text{Co}_{350}(\text{ClO}_4)_2$ with $\text{Co}_{350}\text{DNA}$ and with $\text{Co}_{350}\text{PSS}$. The voltammetry involves oxidation and reduction of the cobalt complex. Voltammetric reduction of Co^{II} to Co^{I} initiates charge transport by electron hopping (bimolecular electron self-exchange).² The rate of physical diffusion is assessed by voltammetric oxidation of Co^{II} to Co^{III} ; electron hopping between these oxidation states is very slow. The two transport rates have allowed us to dissect and fully describe transport in DNA melts. An important conclusion is that on the microscopic level of electron hopping between Co^{II} and Co^{I} , there are two kinds of Co complex in a melt mixture of $\text{Co}_{350}(\text{ClO}_4)_2$ and $\text{Co}_{350}\text{DNA}$ (or $\text{Co}_{350}\text{PSS}$): complexes that have immobile DNA counterions and those that have mobile ClO_4^- counterions (Figure 2). The former are relatively electroinactive and do not support charge transport by Co^{III} electron hopping, owing to the slow time constant of relaxation of their ionic atmosphere. A percolation effect in the $\text{Co}_{350}(\text{ClO}_4)_2$ and $\text{Co}_{350}\text{-DNA}$ mixtures therefore arises. Ultimately, the results extend our understanding of these materials in regard to possible use in molecular electronic environments that incorporate nucleic acid sequence programming. The present results are consistent with recent results¹⁰ on CO_2 -plasticized Co complex melts, and with the notion that immobilization of counterions can produce a large impediment to electron transfer.¹¹

Experimental Section

All reagents for synthesis were purchased from Sigma Aldrich Co. and purified before use. Millipore ultrapure water was used for all experiments. DNA from herring testes (Sigma) was used for all experiments unless otherwise noted. Oligonucleotides were obtained

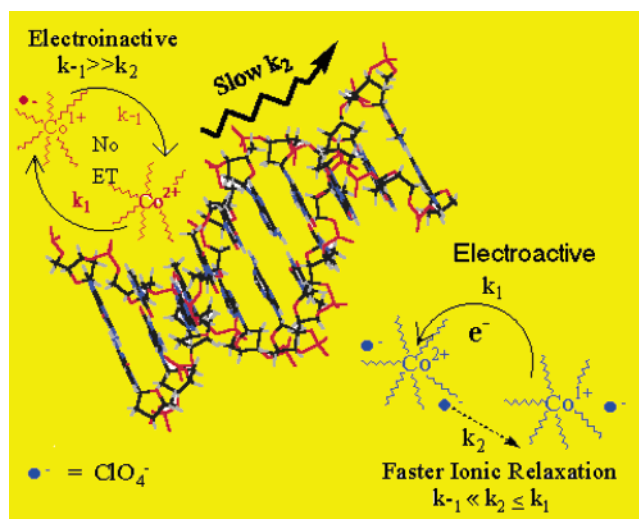


Figure 2. Cartoon of the effects of counterion relaxation on electron hopping in a mixture of $\text{Co}_{350}\text{DNA}$ and $\text{Co}_{350}(\text{ClO}_4)_2$. Two microscopically distinct Co_{350} species are observed experimentally. Co_{350} cations with mobile perchlorate counterions are active in electron-hopping transport, whereas Co_{350} cations having DNA phosphates as counterions are relatively inactive. k_1 and k_{-1} are the forward and reverse electron-transfer rates for the reaction of Co^{I} with Co^{II} . k_2 is the rate of diffusive counterion motion, which for Co complexes with DNA counterions is insignificant compared to k_{-1} , and less than or comparable to k_1 for Co complexes with ClO_4^- (●) counterions. See eq 2.

from MWG-Biotech, Inc. “G oligo” refers to the following sequence: 3′ G-A-T-G-A-A-G-T-G-T-G-A-T-G-T-A-G-A-A-G-A-T-G-T-G 5′ and “A oligo” is as follows: 3′ C-A-C-A-T-C-T-T-C-T-A-C-A-T-C-A-C-A-C-T-T-C-A-T-C 5′. Highly polymerized DNA from calf thymus (CT DNA) was twice phenol-extracted before use. 70 000 MW sulfonated polystyrene (sodium salt) from Aldrich was purified in a 5000 MWCO dialysis membrane as described previously.¹² Elemental analyses were performed by EAI Co. The metal complex molten salt $\text{Co}_{350}(\text{ClO}_4)_2$ (Figure 1) was prepared as previously described.² $\text{Co}_{350}\text{DNA}$ was prepared as described previously⁸ with the modifications described below. A value of $\epsilon = 6600 \text{ M}^{-1} \text{ cm}^{-1}$ at 260 nm was used to determine DNA concentration. Aqueous solutions containing 1.6 equivalents of $\text{Co}_{350}(\text{ClO}_4)_2$ and 2 equivalents of nucleotide were mixed in a 1000 MWCO dialysis tube. The dialysis was intended to remove the perchlorate counterions of the metal complex $\text{Co}_{350}(\text{ClO}_4)_2$ and the native sodium cations of the nucleotide; these small ions cross the membrane more rapidly than does the 2800 molecular weight metal complex. The tubing was placed in a 1-L water reservoir for 96 h at 4 °C. The water was changed every 24 h. The quantity of the Co complex (Co_{350}) that exits was monitored spectrophotometrically by measuring the reservoir absorbance at 306 nm using the determined absorbance coefficient ($31\,700 \text{ M}^{-1} \text{ cm}^{-1}$). The Co complex leaves the dialysis bag slowly enough that the maximum quantity of sodium ions exit before equilibrium is reached (equilibrium being when the Co complex ceases to enter the reservoir because there are no longer any perchlorate counterions to accompany it in permeation). At this point, the dialysis bag contains Co complex and nucleotide in a nearly stoichiometric 1:2 ratio, from which the $\text{Co}_{350}\text{DNA}$ melt is obtained following removal of the water in a vacuum. Elemental: theory for $\text{Co}_{350}\text{DNA}$, C 52.2; H 6.87; N 5.45; Co 1.73; P 1.82; Anal.: C 50.33; H 6.92; N 4.79; Co 2.06; P 1.29; Na 0.016; Cl 0.03.

The Co_{350} melt of sulfonated polystyrene ($\text{Co}_{350}\text{PSS}$) was prepared according to the method just described for $\text{Co}_{350}\text{DNA}$. An average polymer molecular weight of 70 000 g/mol was assumed to quantify anionic sulfonate groups from mass measurement. Elemental: theory

(10) Lee, D.; Hutchison, J. C.; Leone, A. M.; DeSimone, J. M.; Murray, R. W. *J. Am. Chem. Soc.* **2002**, *124*, 9310–9317 (b) Lee, D.; Harper, A. S.; DeSimone, J. M.; Murray, R. W. *J. Am. Chem. Soc.* **2002**, *125*, 1096–1103.

(11) Marcus, R. A. *J. Phys. Chem. B* **1998**, *102*, 10 071–10 077.

(12) Majda, M.; Faulkner, L. R. *J. Electroanal. Chem. Interfacial Electrochem.* **1984**, *169*, 77–95.

for $\text{Co}_{350}\text{PSS}$, C 55.1; H 7.1; N 2.7; Co 1.9; S 2.0; Anal.: C 53.7; H 7.1; N 2.7; Co 1.9; S 1.29; Na 0.016; Cl 0.05.

Molten salts that are mixtures of $\text{Co}_{350}\text{DNA}$ and $\text{Co}_{350}(\text{ClO}_4)_2$ were prepared by mixing solutions of the respective species in molar ratios of 1:0.35, 1:0.6, 1:1, 1:2, 1:3, 1:4, and 1:10. The concentration of the cobalt complex was determined ($\lambda_{\text{max}} = 306$, $\epsilon = 31\,700\text{ M}^{-1}\text{ cm}^{-1}$) by UV spectrophotometry in solutions of $\text{Co}_{350}\text{DNA}$ and $\text{Co}_{350}(\text{ClO}_4)_2$. After thorough mixing of the solution, the water was removed in a vacuum. Molten salts that were mixtures of $\text{Co}_{350}\text{PSS}$ and $\text{Co}_{350}(\text{ClO}_4)_2$ were prepared analogously, by mixing solutions of the respective species in molar ratios of 1:1, 1:2, 1:3, 1:10, and 1:20.

Electrochemical experiments were performed by casting films of the melts onto a three electrode platform as previously described.³ The film was dried at 70 °C under vacuum for at least 12 h prior to analysis and was kept at 67 °C and under 10^{-3} Torr vacuum during voltammetry, which was done with an in-house built low current potentiostat and software. The working microelectrode was a 5.63- μm radius Pt disk, and the reference a silver quasi-reference unless otherwise noted. Diffusion coefficients in the melts were determined chronoamperometrically. The current–time data resulting from potential steps from the foot to the plateaus of the Co^{II} reduction and Co^{III} oxidation waves were plotted according to the Cottrell equation.^{13,14}

Results and Discussion

We have previously shown that samples of heterogeneous DNA, 100–1000 base pairs in length, form molten salt phases of nucleic acids when the native sodium cation is replaced with a polyether-decorated cation.⁸ It was demonstrated that the DNA in the melt remains double stranded. Metal complexes can be chosen according to their redox potentials to selectively oxidize nucleotide bases,^{8,15} and can display electrocatalytic currents in melt phases containing both DNA and a suitable metal complex (Fe, Ru). This paper describes a quantitative study of the charge and mass transport properties of $\text{Co}_{350}\text{DNA}$ and of mixtures of $\text{Co}_{350}(\text{ClO}_4)_2$ and $\text{Co}_{350}\text{DNA}$, along with the effect of nucleic acid size, structure, and base content. Note that with Co complexes, no redox chemistry of the DNA bases is observed; we are therefore studying only the effects of the DNA medium on the Co electrochemistry.

A cyclic voltammogram (Figure 3A) of undiluted $\text{Co}_{350}(\text{ClO}_4)_2$ exhibits two waves. The currents for the Co^{II} reduction wave ($E_{1/2} = -0.79\text{ V}$ vs AgQRE) are larger than those for the Co^{III} oxidation wave ($E_{1/2} = 0.21\text{ V}$ vs AgQRE), because electron hopping reactions augment the rate of charge transport during the reduction.^{2,16,17} The rate of charge transport during the Co^{II} reduction is a summation of the rates of physical diffusion of the Co complex and of electron hopping, or self-exchange, between Co^{II} and Co^{I} states of the complex, according to the Dahms-Ruff relation¹⁸

$$D_{\text{APP}} = D_{\text{PHYS}} + k_{\text{EX}}\delta^2 C/6 \quad (1)$$

where D_{APP} is the experimentally measured diffusion coefficient for the reduction wave, k_{EX} is the rate constant ($\text{M}^{-1}\text{ s}^{-1}$) for

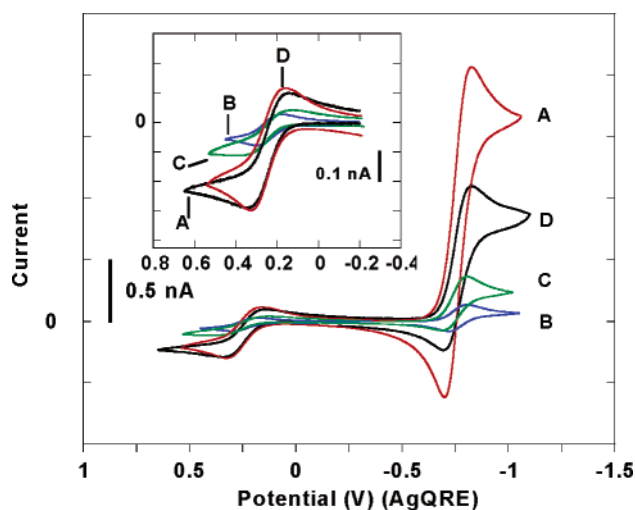


Figure 3. Cyclic voltammetry of (A) pure $\text{Co}_{350}(\text{ClO}_4)_2$ and of mixtures of $\text{Co}_{350}\text{DNA}$ and $\text{Co}_{350}(\text{ClO}_4)_2$ in mole ratios (B) 1:0.6, (C) 1:2 and (D) 1:4, at 10 mV/s at 67 °C under vacuum on a 5.63 μm radius Pt disk microelectrode.

Co^{II} self-exchange, and C and δ are concentration (M) and metal center to center distances (cm), respectively, in the Co_{350} melt. δ is taken as the average or equilibrium center-to-center separation between metal complexes and is calculated from melt density.¹⁹ In contrast, Co^{III} electron self-exchange is extremely slow, so that the oxidation currents are determined solely by physical diffusion of the Co^{II} complex,¹⁷ and provide a measurement of D_{PHYS} in eq 1. The peak current for the reduction of $\text{Co}_{350}(\text{ClO}_4)_2$ is over 6-fold larger than that for oxidation; since peak currents scale with $D^{1/2}$ this means that D_{APP} for the Co^{II} wave is nearly 40-fold larger than D_{PHYS} for the Co^{III} wave in this semisolid melt. Slow physical diffusion of redox polymer hybrid metal complexes is typical in these highly viscous materials and the electron hopping pathway frequently dominates charge transport for the Co^{II} couple,² as it does in Figure 3A.

We did not succeed, on the other hand, in observing cyclic voltammetry in the undiluted $\text{Co}_{350}\text{DNA}$ melt. This melt apparently has an extremely low ionic conductivity, and only highly resistively distorted responses are seen in its voltammetry. This was not entirely surprising since the counterions of the Co complexes are the DNA phosphate sites. At 100 kDa, the massive and relatively inflexible DNA counterion is assumed to be diffusively immobile, so that the phosphates are essentially fixed charged sites.²⁰ The result is a rigid structure unable to support voltammetry. On both traditional macroscopic¹³ and microscopic (ionic relaxation)¹¹ grounds, electroneutrality constraints require physical displacement of the counterion of the

(13) Bard, A. J.; Faulkner, L. R. *Electrochemical Methods*; Second ed.; John Wiley and Sons: New York, 2001.

(14) Laitinen, H. A.; Kolthoff, I. M. *J. Am. Chem. Soc.* **1939**, *61*, 3344 (b) Laitinen, H. A. *Trans. Electrochem. Soc.* **1942**, *82*, 289.

(15) Weatherly, S. C.; Yang, I. V.; Thorp, H. H. *J. Am. Chem. Soc.* **2001**, *123*, 1236–1237.

(16) Kaufman, F. B.; Engler, E. M. *J. Am. Chem. Soc.* **1979**, *101*, 547–549.

(17) Buttry, D. A.; Anson, F. C. *J. Am. Chem. Soc.* **1983**, *105*, 685–689.

(18) Majda, M. In *Molecular Design of Electrode Surfaces*; Murray, R. W., Ed.; John Wiley and Sons: New York, 1992; p 159 (b) Dahms, H. *J. Phys. Chem.* **1968**, *72*, 362 (c) Ruff, I.; Botar, L. *J. Chem. Phys.* **1985**, *83*, 1292.

(19) δ is ordinarily taken as the distance between redox reactants at the instant of electron transfer, which can be less than the equilibrium δ . However, the Co–Lig-tailed complexes may have microscopic motion within the polyether tail shell that achieves close contact between the metal complexes on a time scale shorter than that of the electron-transfer reaction. Thus, the rate constant k_{EX} in these melts may represent a contact reaction. The equilibrium δ is however, the appropriate distance to represent the overall diffusive charge displacement. δ is calculated based on a cubic lattice model. Density ρ , metal complex concentration C , and center-to-center metal spacing δ for **2** are $\rho = 1.12\text{ g/cm}^3$, $C = 0.327\text{ M}$, and $\delta = 17.2\text{ \AA}$, respectively.

(20) Polyether segmental motions however, do not seem to be affected. DSC provides identical glassing temperatures of $-52.4\text{ }^\circ\text{C}$ for all of the materials studied here. This glassing temperature is characteristic of ethylene oxide, but is surprising given the obvious differences in rigidity of the materials. They range from a soft plastic like material for **2** to a viscous liquid for **1**.

Table 1. Summary of Charge Transport and Composition of Co₃₅₀DNA and Co₃₅₀(ClO₄)₂ Melts and Their Mixtures

melt mole ratio Co ₃₅₀ Y: Co ₃₅₀ (ClO ₄) ₂	D _{PHYS} (cm ² /s) ^a	[Co] _{TOTAL} (M)	D _{PHYS} (cm ² /s) ^b	[Co] _{MCI} (M)	D _{APP} (2/1) (cm ² /s) ^b	k _{EX} (M ⁻¹ s ⁻¹) ^c	mass % DNA	mass % PEG	[DNA] (bases, M)
pure Co ₃₅₀ (ClO ₄) ₂	5.3 × 10 ⁻¹⁰	0.44	5.3 × 10 ⁻¹⁰	0.44	2.1 × 10 ⁻⁸	1.2 × 10 ⁷	N/A	70	
1:10, Y=DNA ^e	4.5 × 10 ⁻¹⁰	0.43	5.5 × 10 ⁻¹⁰	0.39	1.3 × 10 ⁻⁸	7.2 × 10 ⁶	1.94	69	0.08
1:4, Y=DNA	4.7 × 10 ⁻¹⁰	0.41	7.2 × 10 ⁻¹⁰	0.33	8.5 × 10 ⁻⁹	4.8 × 10 ⁶	4.20	68	0.16
1:3, Y=DNA	3.5 × 10 ⁻¹⁰	0.40	6.2 × 10 ⁻¹⁰	0.30	6.8 × 10 ⁻⁹	4.0 × 10 ⁶	5.22	67	0.20
1:2, Y=DNA	1.1 × 10 ⁻¹⁰	0.40	2.5 × 10 ⁻¹⁰	0.27	2.8 × 10 ⁻⁹	1.7 × 10 ⁶	6.88	66	0.27
1:1, Y=DNA	2.4 × 10 ⁻¹¹	0.39	9.6 × 10 ⁻¹¹	0.195	7.6 × 10 ⁻¹⁰	4.9 × 10 ⁵	10.1	65	0.39
1:0.6, Y=DNA	1.0 × 10 ⁻¹¹	0.37	7.1 × 10 ⁻¹¹	0.14	2.8 × 10 ⁻¹⁰	1.7 × 10 ⁵	12.4	64	0.46
1:0.35, Y=DNA	(≤1.0 × 10 ⁻¹¹) ^d	0.35	(≤1.5 × 10 ⁻¹⁰) ^d	0.09	(≤1.5 × 10 ⁻¹⁰) ^d	N/A	14.4	63	0.52
pure Co ₃₅₀ DNA	N/A	0.33	N/A	0	N/A	N/A	18.8	61	0.65
1:2, Y= SS G oligo ^f	8.4 × 10 ⁻¹¹	0.40	1.9 × 10 ⁻¹⁰	0.27	1.7 × 10 ⁻⁹	1.0 × 10 ⁶	6.88	66	0.27
1:2, Y= SS A oligo ^f	8.8 × 10 ⁻¹¹	0.40	2.0 × 10 ⁻¹⁰	0.27	1.7 × 10 ⁻⁹	1.0 × 10 ⁶	6.88	66	0.27
1:2, Y=CT DNA ^f	1.3 × 10 ⁻¹⁰	0.40	2.9 × 10 ⁻¹⁰	0.27	1.9 × 10 ⁻⁹	1.1 × 10 ⁶	6.88	66	0.27

^a Calculated from Cottrell slope using total [Co] = ([Co]_{MCI} + [Co]_{FCl}). ^b Calculated from Cottrell slope using [Co]_{MCI}. ^c k_{EX} calculated from D_{APP}(2/1) - D_{PHYS} using eq 1. ^d Diffusion coefficients measured at 82.5 °C. ^e The nucleotide is Herring Testes DNA unless otherwise noted. ^f The nucleotide is SS = single stranded; CT = Calf Thymus.

Co complex for any significant electrochemistry and charge transport, respectively, to occur (Figure 2, $k_{-1} \gg k_2$).

In our previous study,⁸ the Co₃₅₀DNA melt that was prepared contained excess Co₃₅₀(ClO₄)₂ due to use of a 100 MWCO dialysis bag that did not allow permeation of the Co complex (see the Experimental Section). The resulting increment of mobile ions remaining in this less pure⁸ Co₃₅₀DNA melt allowed observations of voltammetric behavior that proved not to be possible in the present, more highly purified Co₃₅₀DNA melt material. To observe voltammetry in the present studies, we added controlled amounts of Co₃₅₀(ClO₄)₂ to the purified Co₃₅₀DNA melt.

Addition of 0.35 equivalents of Co₃₅₀(ClO₄)₂ to the Co₃₅₀DNA melt (1:0.35 Co₃₅₀DNA:Co₃₅₀(ClO₄)₂) provided a sufficient increment of ionic conductivity to support voltammetry (see the Supporting Information), at least at temperatures exceeding 80 °C. The physical diffusivity of the Co complex was estimated as D_{PHYS} ≤ 1.0 × 10⁻¹¹ cm²/s. With higher added increments of Co₃₅₀(ClO₄)₂, voltammetry was achievable at 67 °C, such as in Figure 3B where 0.6 equiv of Co₃₅₀(ClO₄)₂ have been added to the Co₃₅₀DNA melt. Two changes, relative to Figure 3A (also measured at 67 °C), are seen. First, oxidation and reduction currents in Figure 3B are both smaller than those in Figure 3A, that is, the charge transport rates obtained from the oxidation (D_{PHYS}) and reduction (D_{APP}) waves are both smaller in the 1:0.6 Co₃₅₀DNA:Co₃₅₀(ClO₄)₂ mixture, as compared to the pure Co₃₅₀(ClO₄)₂ melt. Second, the effect on D_{APP} is much larger than on D_{PHYS}; Figure 3, parts A and B, show 1:6 vs 1:2 ratios of the oxidation and reduction currents. Voltammograms for addition of further increments of Co₃₅₀(ClO₄)₂ to the Co₃₅₀DNA melt, up to a mole ratio of 1:4 Co₃₅₀DNA:Co₃₅₀(ClO₄)₂, are shown in Figure 3, parts C and D. Values of D_{PHYS} and D_{APP} measured by chronoamperometry for the mixtures of Co₃₅₀(ClO₄)₂ and Co₃₅₀DNA are given in Table 1. The data show a steady increase in both D_{PHYS} and D_{APP} (read the table from pure Co₃₅₀DNA upward to pure Co₃₅₀(ClO₄)₂), as greater quantities of Co₃₅₀(ClO₄)₂ are added to the Co₃₅₀DNA.²¹

Consider the variations in D_{PHYS} first. (Ignore for the moment that Table 1 shows two sets of D_{PHYS} results; this is associated with what is used for the concentration of diffusing Co^{II}, as

discussed below.) Table 1 shows that D_{PHYS} varies relatively little at higher added proportions of Co₃₅₀(ClO₄)₂, but falls sharply for Co₃₅₀DNA:Co₃₅₀(ClO₄)₂ mole ratios lower than 1:3. The main effects thus seem to be operative at lower proportions of Co₃₅₀(ClO₄)₂; there are plausibly three effects: (i) Adding mobile ClO₄⁻ counterions to the Co₃₅₀DNA melt allows ionic current between the electrodes, and relaxes electroneutrality constraints on oxidizing Co^{II} to Co^{III} (through ClO₄⁻ transport toward the working electrode). Ionic migration enhancement of D_{PHYS} may also occur; this would have the largest relative effect on D_{PHYS} at low proportions of added Co₃₅₀(ClO₄)₂. (ii) Adding Co₃₅₀(ClO₄)₂ to the Co₃₅₀DNA melt also adds PEG content, which should plasticize physical diffusion as seen before in Co poly-pyridine-PEG molten salts.²² This effect should be minor, however, because the increase in mass percentage of PEG (Table 1) is only from 63 to 65% as the mole ratio changes from 1:0.35 to 1:1. (iii) Although the DNA strands are massive, the molar volume of an *individual* base pair is less than one-third of that of the Co complex (PEG tails included). The Co concentration is thus only modestly diluted by the DNA as seen by examining the [Co]_{TOTAL} column in Table 1. The DNA macromolecule undoubtedly nonetheless provokes some tortuosity-based depression of the Co complex diffusion rate, and this should occur for the melt mixtures with the largest mole fractions of DNA polyanions, which is where the largest variations in D_{PHYS} in fact occur.

The pattern of variation of D_{APP} for the Co^{III} reaction (labeled D_{APP}(2/1) in Table 1) with Co₃₅₀(ClO₄)₂ content in Co₃₅₀DNA:Co₃₅₀(ClO₄)₂ melt mixtures differs from that of D_{PHYS}. Although D_{PHYS} changes most strongly with Co₃₅₀(ClO₄)₂ content at low proportions of Co₃₅₀(ClO₄)₂, the changes in D_{APP}(2/1) values are largest at *high* proportions of Co₃₅₀(ClO₄)₂ (Table 1). Between pure Co₃₅₀(ClO₄)₂ and mixtures with a 1:4 mole ratio of Co₃₅₀DNA:Co₃₅₀(ClO₄)₂, D_{APP}(2/1) falls 3-fold; D_{PHYS} changes by <10% over that range. D_{APP}(2/1) decreases ~140-fold from pure Co₃₅₀(ClO₄)₂ to 1:0.35 mole ratio Co₃₅₀DNA:Co₃₅₀(ClO₄)₂. That is, the rate constants (k_{EX} in Table 1) of Co^{III} electron hopping transport become substantially depressed when the Co complex counterion is changed from ClO₄⁻ to DNA. How does DNA so profoundly suppress the Co^{III} electron hopping flux and k_{EX}? The electron hopping rate should be slowed by lowered Co complex concentrations, but the overall

(21) The fact that the Co^{III} waves exhibit significantly greater radial character as the proportion of Co₃₅₀(ClO₄)₂ increases, illustrates the role of diffusion in affecting the observed current changes of Figure 3.

(22) Crooker, J. C.; Murray, R. W. *Anal. Chem.* **2000**, *72*, 3245–3252.

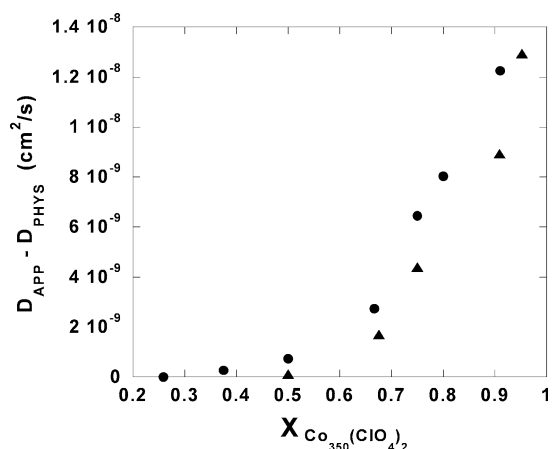


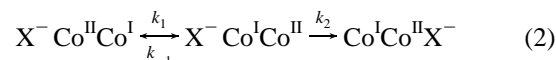
Figure 4. Dependence of $D_{\text{APP}} - D_{\text{PHYS}}$ on (●) the mole fraction of $\text{Co}_{350}(\text{ClO}_4)_2$ in mixtures of $\text{Co}_{350}\text{DNA}$ and $\text{Co}_{350}(\text{ClO}_4)_2$, and (▲) on the mole fraction of $\text{Co}_{350}(\text{ClO}_4)_2$ in mixtures of $\text{Co}_{350}\text{PSS}$ and $\text{Co}_{350}(\text{ClO}_4)_2$, where PSS is sulfonated polystyrene.

dilution by the DNA is modest, as noted above. For the same reason, and especially when the proportions of $\text{Co}_{350}(\text{ClO}_4)_2$ in the mixture melt are high, electron tunneling-based slowing of electron transfers by DNA-enforced separations between the Co complexes should be minor.

It is in fact difficult to rationalize the strong variation of Co^{III} electron hopping rates, especially at high mole fractions of $\text{Co}_{350}(\text{ClO}_4)_2$ unless *not all of the Co complex centers participate in electron transport by Co^{III} self-exchange reactions*. We propose that the portion of Co complexes that have fixed-charged site DNA phosphate counterions are inactive, or effectively inactive, in transport by Co^{III} electron hopping. There is a sound basis¹⁰ for this hypothesis as explained below. The Co complexes having more mobile ClO_4^- counterions are active in transport. Labeling these two different “kinds” of complexes Co_{FCI} and Co_{MCI} , for “fixed” counterion and mobile counterion, respectively, we define the mole fraction of the latter (relative to total Co complex concentration in each mixture) as X_{Co} . Thus, in a series of $\text{Co}_{350}\text{DNA}:\text{Co}_{350}(\text{ClO}_4)_2$ melt mixtures, the proposed picture is that the electron transport-active Co_{MCI} complex sites become replaced with electron transport-inactive Co_{FCI} sites, which act as transport-blocking sites.

The preceding paragraph describes a classical static percolation situation, and it would accordingly be expected that the value of $((D_{\text{APP}} - D_{\text{PHYS}}) \propto k_{\text{EX}})$ should decrease with decreasing X_{Co} down to a critical percolation threshold, below which the electron hopping reaction would be very slow. Figure 4 plots the results from Table 1 in this way, using D_{APP} values calculated using the concentration $[\text{Co}]_{\text{MCI}}$ (●). Figure 4 in fact illustrates typical percolation behavior, with a threshold near 0.5. Percolation behavior has been previously detected⁴ in redox polyether hybrid melts, in which $\text{Fe}^{\text{III/II}}$ PEG-tailed-polypyridine complex sites, which are active toward electron hopping, were replaced with inactive Co^{III} ones, so it is known that these materials are sufficiently rigid to display percolation properties.²³

The percolation effect (Figure 4) rationalizes the concentration dependence of Co^{III} electron transport; we next address the relative inactivity of Co complexes with DNA counterions in electron transport. There are at least two possibilities. In one, the Co^{III} electron self-exchange is slowed by strong ion-pairing, of phosphate relative to perchlorate. The second possibility is less speculative, more likely, and consistent with other recent results.¹⁰ Any Co^{III} electron-transfer reaction in the semisolid melt produces a local Coulombic displacement that requires a preceding, or following microscopic displacement or reorganization of ionic charge.¹¹ Said differently, the local ionic atmosphere of the reaction pair must relax. The reaction can be written as



where the X^- counterion has a diffusive time constant (k_2^{-1}) that describes its microscopic displacement. When the counterion is a DNA base pair, the counterion displacement time constant k_2^{-1} will be very long (compared to that for ClO_4^-), with the result that back reaction (k_{-1}) of an electron hop becomes important (Figure 2). That is, the Co^{III} back reaction negates any contribution to net electron transfer and to electron transport. We have previously discussed¹⁰ the importance of counterion mobility in $\text{Co}_{350}(\text{ClO}_4)_2$ melts that have been plasticized by CO_2 , showing that the experimental net electron-transfer rate constant is proportional to the diffusion rate of the ClO_4^- counterion, and that $D_{\text{E}} \approx D_{\text{COUNTERION}}$.¹⁰ There is no reason to doubt that this control of the electron-transfer rate by ionic atmosphere relaxation would be less important in the present case of a PEG-tailed Co complex having DNA counterions. A Co^{III} reaction pair with an immobile (DNA) counterion should thus display a slow or negligible contribution to electron transport. The slow electron hopping rate of the $\text{Co}_{350}\text{DNA}$ sites relative to the faster rate of the $\text{Co}_{350}(\text{ClO}_4)_2$ sites create the percolation behavior of Figure 4. The Figure 4 decrease in D_{APP} as $\text{Co}_{350}(\text{ClO}_4)_2$ is added to the $\text{Co}_{350}\text{DNA}:\text{Co}_{350}(\text{ClO}_4)_2$ melt mixture does not require any effect that slows the intrinsic electron hopping rate for the Co_{MCI} species; the decrease is solely explained by the percolative dilution with inactive Co_{FCI} sites.

Comparison of the shape of Figure 4 would be desirable but is complicated by: (a) The blocker sites are linked together, which is an unusual percolation situation. Some computations were done (see the Supporting Information) to compare blocking by 3-mers with nonlinked blocker sites. Although the results were similar, they were not identical. Both were roughly similar to Figure 4. (b) Effects of migration on the curve shape have been neglected; these may be significant at low $\text{Co}_{350}(\text{ClO}_4)_2$ concentrations. (c) Although electron tunneling effects on electron transport are not a major factor, they may influence the shape of Figure 4. A quantitative analysis of Figure 4 is thus somewhat daunting.

We conclude this section with a necessary digression. The D_{APP} values and corresponding electron-transfer rate constants in Table 1 were calculated using the concentrations of $\text{Co}_{350}(\text{ClO}_4)_2$ (i.e., $[\text{Co}]_{\text{MCI}}$), rather than total Co concentration. In calculating D_{PHYS} , whether one uses $[\text{Co}]_{\text{MCI}}$ or $[\text{Co}]_{\text{TOTAL}}$ depends on whether Co complexes associated with the DNA phosphate counterions can exchange places with $\text{Co}_{350}(\text{ClO}_4)_2$

(23) Blaich, D. N.; Saveant, J.-M. *J. Am. Chem. Soc.* **1992**, *114*, 3332–3340 (b) Electron hopping percolation in redox systems has been modeled^{23a} and a number of potentially complicating chemical features discussed.⁴ Added to those in the present case is the fact that the DNA-associated inactive Co complexes are not randomly distributed, but will be present in chains, organized by the polyanion (DNA in this case, or sulfonated polystyrene in the $\text{Co}_{350}\text{PSS}$ case).

Table 2. Summary of Charge Transport and Composition of Co₃₅₀PSS Melts

melt mole ratio Co ₃₅₀ PSS: C ₃₅₀ (ClO ₄) ₂	D_{PHYS} (cm ² /s) ^a	[Co] _{TOTAL} (M)	D_{PHYS} (cm ² /s) ^b	[Co] _{MCI} (M)	D_{APP} (cm ² /s) ^b	k_{EX} (M ⁻¹ s ⁻¹) ^c	mass % PSS	mass % PEG
pure Co ₃₅₀ (ClO ₄) ₂	5.3×10^{-10}	0.44	5.3×10^{-10}	0.44	2.1×10^{-8}	1.2×10^7	N/A	70
1:20	7.7×10^{-10}	0.44	8.1×10^{-10}	0.42	1.4×10^{-8}	7.5×10^6	0.6	69.9
1:10	2.0×10^{-10}	0.44	5.5×10^{-10}	0.40	9.1×10^{-9}	5.0×10^6	1.1	69.8
1:3	1.3×10^{-10}	0.40	2.7×10^{-10}	0.30	4.5×10^{-9}	2.7×10^6	3.0	69.1
1:2	1.0×10^{-10}	0.37	2.1×10^{-10}	0.25	1.8×10^{-9}	1.1×10^6	4.0	68.8
1:1	3.4×10^{-11}	0.35	9.4×10^{-11}	0.175	1.5×10^{-10}	4.1×10^4	6.0	68.2

^a Calculated from Cottrell slope using total [Co] = ([Co]_{MCI} + [Co]_{FCl}). ^b Calculated from Cottrell slope using [Co]_{MCI}. ^c k_{EX} calculated from $D_{\text{APP}}(2/1) - D_{\text{PHYS}}$ using eq 1.

complexes rapidly compared to the experimental *physical diffusion* time scale. If not, then the concentrations [Co]_{MCI} should be used to calculate D_{PHYS} from the Cottrell plot slopes (see Table 1, $D_{\text{PHYS,MCI}}$). If, however, the exchange of Co_{MCI} with Co_{FCl} is rapid on the experimental *physical diffusion* time scale, the total concentration [Co]_{TOTAL} should be used (see Table 1, D_{PHYS} column). We believe this latter picture is the better choice and is supported by Figure 3 where both [Co]_{TOTAL} and the currents for the Co^{III/II} waves are nearly identical in the Co₃₅₀(ClO₄)₂ and (1:4 Co₃₅₀DNA:Co₃₅₀(ClO₄)₂) melts (Figure 3, parts A and D, respectively). Additionally, previous observations in analogous melts⁸ of an EC reaction between DNA and Fe₃₅₀(ClO₄)₂ (Fe homologue of Co₃₅₀(ClO₄)₂) indicate that electrochemically generated Fe^{III} complexes are transported to DNA fixed counterion sites. This process is not accompanied by preferential binding of the higher-valent metal complex because there were no shifts in $E_{1/2}$ or differences between anodic and cathodic peak currents for either of the Co waves.²⁴ We argue accordingly that D_{PHYS} values based on [Co]_{TOTAL} are more accurate.

Other Counterions to Co Complex. The above experiments were expanded to include other Co₃₅₀ Y counterions where Y was a nucleic acid varied as to size, base content, and structure, and to a nonbiological example, sulfonated polystyrene. The experiments with nucleic acids used melt mixtures containing 1:2 mole ratios of Co₃₅₀Y to Co₃₅₀(ClO₄)₂—a proportion that allows facile voltammetric analysis but retains a high nucleic acid concentration. Two Co₃₅₀ counterions used were synthetic 25-mer oligonucleotides, one being a guanine-rich sequence, “G oligo” and the other its complementary sequence, “A oligo” containing no guanines (see the Experimental Section for oligonucleotide sequences). The charge transport results from the two single stranded DNA melts (Y = SS G oligo and SS A oligo) produced from these two short sequences are given in Table 1 (bottom). DNA melts from highly polymerized calf thymus (CT) DNA were also investigated.

DNA lengths from 0.025 to 10³ kBP, both single and double-stranded DNA, and a strong variation in base content are represented among the above materials. Despite these variations, Table 1 shows that all the materials give nearly identical results for D_{PHYS} and D_{APP} , including the 1:2 Co₃₅₀DNA:Co₃₅₀(ClO₄)₂ melt in the upper part of Table 1. This finding emphasizes that it is the immobile counterion aspect of DNA that defines the transport characteristics of these materials, especially for D_{APP} (2/1).

The theme of an immobile poly-counterion was extended to polystyrene sulfonate (Figure 1, PSS). The 70 000 MW PSS

polyanion is similar in size to DNA, but has a much less complex structure. Faulkner¹² studied films of PSS as a water swollen cation exchanger, to contrast their properties to those of the more intricately structured Nafion films.^{17,25,26}

Melts that are mixtures of Co₃₅₀PSS and Co₃₅₀(ClO₄)₂ were prepared and subjected to chronoamperometric determination of D_{PHYS} (from the Co^{III/II} wave) and D_{APP} (from the Co^{II/I} wave). The results (Table 2) exhibit the same trends as the Co₃₅₀ DNA materials. D_{PHYS} changes most strongly at low Co₃₅₀(ClO₄)₂ content, whereas D_{APP} changes occur mostly at high Co₃₅₀(ClO₄)₂ content. If Co₃₅₀PSS is inactive for Co^{II/I} electron transport (like Co₃₅₀DNA), then the Co₃₅₀PSS:Co₃₅₀(ClO₄)₂ mixtures should also display a static percolation behavior. Figure 4 (▲) shows that this indeed occurs, with a threshold (ca. 0.5) identical to that for the Co₃₅₀ DNA mixtures (●). Further, the numerical values of $D_{\text{APP}} - D_{\text{PHYS}}$ are very similar in the two different kinds of melts. The similarity implies that the ionic atmosphere relaxation control of Co^{II/I} electron transfer for the Co₃₅₀(ClO₄)₂ component of the melt mixture is relatively indifferent to the nature of the inactive Co₃₅₀ Y sites. The sulfonated polystyrene and nucleic acid variation experiments illustrate the pronounced influence of slow ionic atmosphere relaxation on electron transport characteristics in these phases.

Conclusions

Numerous studies of charge transport and electron transfer have considered the effects of structural heterogeneity within ion exchange polymer films^{12,24,25} containing ionic redox species. These films were contacted by fluid solvent containing a dissolved supporting electrolyte, so that the film could be permeated by mobile electrolyte ions and swollen by the solvent.

The present work shows that redox sites that have large counterions such as DNA or PSS are rendered inactive in electron transport. This behavior seems to be a generic one given the similarity of results for nucleic acids and PSS and leads to a static percolative behavior when the relative amounts of perchlorate and Y present are varied. Based on other work¹⁰ on Co₃₅₀(ClO₄)₂ melts, the net electron-transfer rates and Co^{II/I} electron transport are controlled by a kind of solvent dynamics control involving relaxation of the surrounding ionic atmosphere, notably by the rate of diffusive motions of the ClO₄⁻ counterions as the k_2 step in eq 2. Thus, the values of k_{EX} cited in Tables 1 and 2 are *not* the intrinsic electron self-exchange rate constants of the Co complex II/I couple, but are rather lower limits of

(24) Carter, M. J.; Bard, A. J. *J. Am. Chem. Soc.* **1987**, *109*, 7528–7530 (b) Carter, M. T.; Rodriguez, M.; Bard, A. J. *J. Am. Chem. Soc.* **1989**, *111*, 8901.

(25) Vining, W. J.; Meyer, T. J. *J. Electroanal. Chem.* **1987**, *237*, 191–208 (b) Anson, F. C.; Blauch, D. N.; Saveant, J. M.; Shu, C. F. *J. Am. Chem. Soc.* **1991**, *113*, 1922–1932.
(26) Buttry, D. A.; Anson, F. C. *J. Am. Chem. Soc.* **1982**, *104*, 4824–4829 (b) Rubinstein, I.; Bard, A. J. *J. Am. Chem. Soc.* **1980**, *102*, 6641–6642 (c) Rubinstein, I. *J. Electroanal. Chem.* **1985**, *188*, 227–244 (d) Buttry, D. A.; Saveant, J. M.; Anson, F. C. *J. Phys. Chem.* **1984**, *88*, 3086–3091.

those rate constants. Notably, the rate constant for the $\text{Co}^{\text{II/I}}$ bipyridine complex in dilute fluid solution is $10^9 \text{ M}^{-1}\text{s}^{-1}$.²⁷

It is interesting that, in principle, one could employ patterns of poly-ions such as DNA to “write” nonconducting pathways in semisolid molecular melt materials.

Acknowledgment. We thank Luke Zannoni for DSC measurements and Dr. John C. Hutchison for many helpful

discussions. This work was sponsored by the Department of Defense under Contract No. DAMD17-98-1-8224 (H.H.T.), and the Department of Energy Division of Basic Sciences (R.W.M.).

Supporting Information Available: Voltammetry of undiluted $\text{Co}_{350}\text{DNA}$ and $\text{Co}_{350}(\text{ClO}_4)_2$ in the mole ratio 1:0.35, voltammetry of undiluted mixtures of $\text{Co}_{350}(\text{ClO}_4)_2$ and $\text{Co}_{350}\text{-PSS}$, information on percolation simulations. This material is available free of charge via the Internet at <http://pubs.acs.org>.

(27) Brunschwig, B. S.; Creutz, C.; Macartney, D. H.; Sham, T. K.; Sutin, N. *Faraday Discuss. Chem. Soc.* **1982**, *74*, 113–127.

JA0348795